

Enhancement of Immunotoxin Efficacy by Acid-cleavable Cross-linking Agents Utilizing Diphtheria Toxin and Toxin Mutants*

(Received for publication, March 30, 1989)

David M. Neville, Jr.†, Kasturi Srinivasachar, Roger Stone, and Joshua Scharff

From the Laboratory of Molecular Biology, National Institute of Mental Health, Bethesda, Maryland 20892

We have utilized a new class of acid-cleavable protein cross-linking reagents in the construction of antibody-diphtheria toxin conjugates (Srinivasachar, K., and Neville, D. M., Jr. (1989) *Biochemistry* 28, 2501-2509). The potency of anti-CD5 conjugates assayed by inhibition of protein synthesis on CD5 bearing cells (Jurkat) is correlated with cross-linker hydrolytic rates. The maximum increase in potency of the cleavable conjugates over non-cleavable conventional conjugates is 50-fold and is specific for the CD5 uptake route as judged by competition with excess anti-CD5. The potency of conjugates made from diphtheria toxin and the anti-high molecular weight melanoma-associated antigen (HMW-MAA) is enhanced 3-10-fold by a cleavable cross-linker. However the potency of transferrin or anti-CD3 diphtheria toxin conjugates is only minimally enhanced (2-3-fold).

Mutant diphtheria toxins, CRM103 and CRM9, previously shown to express less than $\frac{1}{100}$ of the wild type in binding affinity were substituted into these conjugates as probes for possible intracellular toxin receptor interactions. Both mutants were equally as toxic to Jurkat target cells exhibiting $\frac{1}{100}$ the wild-type potency. CRM9 non-cleavable conjugates were equally as potent as wild-type conjugates for transferrin and anti-CD3-mediated uptake but not for anti-CD5-mediated uptake where toxicity was reduced 60-fold over the wild-type analog. The cleavable cross-linker enhanced the toxicity of anti-CD5-CRM103 and anti-CD5-CRM9 conjugates, but potency was only $\frac{1}{10}$ that of the analogous wild-type cleavable conjugate.

These data are consistent with a model in which potentiation of toxicity of the anti-CD5 and anti-high molecular weight melanoma-associated antigen conjugates by the cleavable cross-linker occurs from an enhanced intracellular toxin-toxin receptor interaction that ultimately results in increased toxin translocation to the cytosol compartment. In contrast, these data indicate that the anti-CD3 and transferrin uptake systems do not require this interaction in agreement with previous work (Johnson, V. G., Wilson, D., Greenfield, L., and Youle, R. J. (1988) *J. Biol. Chem.* 263, 1295-1300).

achieved by coupling a monoclonal antibody (or some other cell surface binding moiety) to a protein toxin or to a toxin fragment. Immunotoxins are designed specifically to kill targeted cells in a mixed cell population. As originally conceived the receptor binding chain of a toxin (B chain), such as ricin or diphtheria toxin, was to be replaced by a new binding moiety, which would direct enzymatically active toxin A chain into a unique cell population having receptors for the modified toxin. It was postulated that hybrid toxins would function as toxin analogs and would retain the unique membrane translocation function of the toxins to the cytosol compartment necessary for the inhibition of cellular protein synthesis (1). A large number of immunotoxins have been constructed utilizing a variety of binding moieties and a variety of holotoxins, toxin A chains, and A chains plus various portions of the B chain (2). Some of these have proven effective *in vitro* for the elimination of targeted cells from mixed cell populations. Applications have included the selection of cells carrying mutated cell surface epitopes (3) and the depletion of T cells from donor bone marrow grafts for the prevention of morbid graft *versus* host disease (4). However, immunotoxins to date have had limited effectiveness as clinical or experimental agents *in vivo* (2, 5). Our view has been that this lack of *in vivo* efficacy is due to the fact that B chain domains necessary for efficient toxin translocation (and therefore specific cell killing) also impart significant toxicity to non-target cells. For a variety of reasons this non-target cell toxicity is more difficult to obviate *in vivo* than *in vitro* (5).

This laboratory has had a long-term interest in defining the determinants of immunotoxin efficacy. We first reported that diphtheria toxin A chain and ricin A toxin conjugates exhibited low cell-killing efficacy (6, 7). Efficacy was partially restored by inclusion of the entire B chain within these conjugates. With ricin conjugates we found that the B chain domain necessary for maximal efficacy included a functional lactose binding site. We proposed that an intracellular ricin binding site was necessary for maximal efficacy even though cellular entry was mediated by an alternate receptor (8). Supporting evidence for this thesis has appeared from a number of investigations (9-11). It is still not clear, however, whether the intracellular ricin receptor interaction represents an efficacious routing to the site of processing and/or translocation or whether the receptor interaction is directly tied to membrane translocation.

Numerous publications have addressed the question as to which B chain domain(s) are necessary for diphtheria toxin conjugate efficacy (12-17). The methodology has been to construct toxin conjugates having either large deletions or point mutations in the toxin binding site. Conjugated hormones, lectins, growth factors, and monoclonal antibodies to cell surface epitopes have dictated the alternate uptake route. The potency of these conjugates has been compared with

Immunotoxins are toxins with altered receptor specificity,

* The costs of publication of this article were defrayed in part by the payment of page charges. This article must therefore be hereby marked "advertisement" in accordance with 18 U.S.C. Section 1734 solely to indicate this fact.

† To whom correspondence should be addressed: Laboratory of Molecular Biology, National Institute of Mental Health, 9000 Rockville Pike, Bldg. 36, Rm. 1B-08, Bethesda, MD 20892. Tel.: 301-496-6807; Fax: 301-496-9935.

intact toxin conjugates. From one such study utilizing DT¹ binding site point mutations the claim was advanced that the receptor binding function of the B chain is not necessary for maximal translocation efficacy (16, 17). However, the data presented in support of this claim were limited to uptake processes mediated by either the transferrin receptor or the T cell epitope CD3. In the case of a study utilizing *Pseudomonas* exotoxin A the claim was also made that the domain mediating toxin binding to surface receptors and the domain mediating toxin translocation are completely separable (18). However, the published data (19) show wide changes between the toxicity of conjugates constructed with intact toxin and a reduced binding truncated form of the toxin, PE40. These changes vary by uptake route.

In the present study we approach the question of internal toxin receptors and immunotoxin efficacy with a new methodology, the use of mild acid-cleavable cross-linking reagents. The rationale that led to this approach is as follows. If one postulates that a unique toxin B chain domain must interact with an internal cellular binding structure (receptor), either for efficacious routing productive in toxicity or directly in the translocation process, then this interaction might be diminished by the antibody or other ligand involved in the conjugation process. If the conjugation was made with a cross-linker cleavable within the endosome, free toxin would be deposited there and the essential interaction would be enhanced over a conventional non-cleavable conjugate. If the essential toxin internal receptor interaction involved the toxin binding site, which also binds surface membrane receptors (as postulated for ricin immunotoxins), then the therapeutic window between target and non-target cells could be enlarged by constructing the immunotoxin so that the toxin binding site was sterically blocked to the highest degree possible prior to cross-linker cleavage. On the other hand, if the toxin surface membrane binding site was not essential internally, the site could be irreversibly blocked either chemically (8) or by the use of toxin binding site mutants (16). Thus a series of toxin conjugates constructed with cleavable and non-cleavable cross-linkers, and with both wild-type and toxin binding site mutants, and utilizing a variety of receptor mediated uptake routes could serve as probes for internal receptor toxin interactions along the toxin translocation pathway.

In the present study we have constructed a series of conjugates based on diphtheria toxin and diphtheria toxin binding site mutants CRM103 (16) and CRM9 (20) utilizing acid-cleavable and non-cleavable cross-linkers. Immunotoxins directed at T cell antigens CD5 and CD3 (CD3 and CD5, T cell surface membrane epitopes) and the high molecular weight melanoma-associated antigen (HMW-MAA) as well as transferrin toxin conjugates have been utilized. The potency and efficacy of these conjugates have been assayed on the appropriate receptor bearing target cells by the inhibition of protein synthesis.

The synthesis of a new class of acid-cleavable protein cross-linking reagents based on orthoester, acetal, and ketal functionalities has been described (21). The unique feature of these functionalities is that their observed hydrolytic rate constants increase 10-fold for each unit drop in pH, a consequence of specific H₃O⁺ catalysis leading to a carbonium ion intermediate (22). Moreover, these functionalities are resistant to base catalysis permitting manipulation and storage at alkaline pH. The cross-linking reagents react with proteins

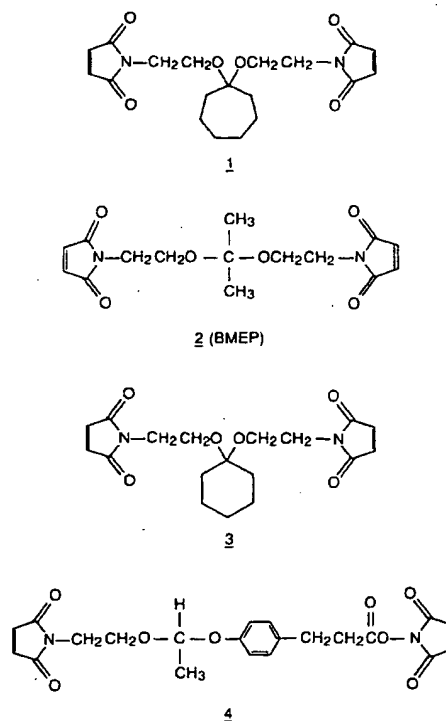


FIG. 1. The structures of acid-cleavable cross-linkers used in this study are shown above. Hydrolytic rates are detailed in Fig. 2 and Table I and decrease in ascending numerical order. BMEP, bis-maleimidoethoxy propane.

via heterobifunctional groups (maleimide and *N*-hydroxysuccinimide ester) or homobifunctional groups (bis-maleimide). The maleimide cross-linking is accomplished by prior protein thiolation with iminothiolane. Cross-linked proteins exhibit first-order dissociation under acid conditions. The *t*_{1/2} at pH 5.5 varies between 0.1 and 130 h for a series of six different cleavable cross-linkers (21). In the present study we have largely used ketal cross-linkers. Acid-catalyzed hydrolysis breaks both O-C-O bonds at the central carbon, generating the parent ketone and 2 mol of the maleimidoethyl alcohol.

MATERIALS AND METHODS

Synthesis of Cross-linkers—Compounds 1 and 3 (Fig. 1) were synthesized from the corresponding diethyl ketals by acid-catalyzed ketal exchange with *N*-(2-hydroxyethyl)maleimide as described previously for compound 2 (16). The NMR spectral data for these compounds are in accord with their structure. Both 1 and 3 are crystalline compounds with melting points 102–104 and 113–114 °C, respectively.

Mutant Toxins—CRM9 was produced from *Corynebacterium diphtheriae* strain C7 (β^h tox-201 tox-9 h) obtained from Dr. Randall K. Holmes, Department of Microbiology, Uniformed Health Services, Bethesda, MD. A mutant toxin strain producing CRM103 (23) was obtained from Dr. Neal Groman, Department of Microbiology, University of Washington. Mutant toxins were grown in the NIH Pilot Plant by Dr. Joseph Shiloach in small fermentors using low iron C-Y media previously described (24, 25) with the exception that the deferration step was omitted. Iron was scavenged by Chelex 100 treatment² and replenished at 0.075 μ g/ml (26). Culture conditions were as described for optimal toxin production for C7 β strains of corynebacteria (25, 26). CRM9 was produced in good yields (~20 μ g/ml culture medium) probably as a consequence of an additional mutation rendering toxin production independent of iron (26).² Mutant toxins were nicked (>90%) with trypsin following purification as described for wild-type toxin. Mutant toxins were additionally purified by size exclusion over GF-250 columns (Du Pont-New England Nuclear). Wild-type toxin

¹ The abbreviations used are: DT, diphtheria toxin; SMPB, succinimidyl-4-(*p*-maleimidophenyl) butyrate; BMH, bis-maleimidohexane; TfR, transferrin receptor; HMW-MAA, high molecular weight melanoma-associated antigen; SDS, sodium dodecyl sulfate.

² R. Holmes, personal communication.

was obtained in nicked form from Connaught Laboratories (Toronto). In a guinea pig assay the minimum lethal dose of CRM9 was found to be 200 times that of wild-type toxin.

Synthesis of Conjugates—Conjugates were synthesized and characterized as described previously (21). T101, a murine anti-human T cell monoclonal IgG reactive with the human T cell CD5 epitope, was a gift of Hybritech (San Diego). SV10016, a monoclonal IgG reactive with HMW-MAA (27) was a gift of Dr. Soldano Ferrone, Department of Microbiology and Immunology, New York Medical College, Valhalla, NY. UCHT1 a monoclonal IgG reactive against the human T cell epitope CD3 was purchased from Oxoid USA, Inc., Charlotte, NC. Toxins and antibody were derivatized with 1–2 thiol group/mol using iminothiolane (Pierce Chemical Co.) and freed of excess reagent by G-25 fine (Pharmacia LKB Biotechnology Inc.) chromatography. Cross-linkers 1, 2, 3 or BMH (Pierce Chemical Co.) in 15-fold excess over thiol were added to the thiolated toxin at pH 8.5 resulting in a derivatization of ~1 free maleimide residue per mol following G-25 fine chromatography. Derivatized antibody and toxins in excess were combined for 45 min and the conjugate product was purified by size exclusion using a GF-250 column (Du Pont-New England Nuclear) at pH 8.5 in 90 mM Na₂SO₄, 10 mM NaH₂PO₄, 1 mM disodium EDTA. All conjugates produced indistinguishable chromatograms and were fractionated identically (21). The average composition of these conjugates determined from hydrolysis of cleavable conjugates was found to be 1 mol of DT per mol of IgG. The heterobifunctional non-cleavable cross-linking reagent SMPB was obtained from Pierce Chemical Co. and conjugation was carried out as described previously (21).

Determination of Half-time of Hydrolysis—These were determined as described previously (21). Following pH reduction, chromatography at different times on GF-450 column (Du Pont-New England Nuclear) in the presence of SDS resolved conjugate, toxin, and antibody peaks utilizing UV detection fed to an integrator. The fraction hydrolyzed was referenced to the maximum hydrolyzed. Generally over 85% of the initial conjugate peak was hydrolyzed.

Protein Synthesis Inhibition Assays—These were performed at 37 °C in RPMI medium plus 0.1% bovine serum albumin as described previously utilizing a 45-min pulse of [¹⁴C]-leucine at the end of the incubation (21). Points are averages of six replicates. When toxin/conjugate exposure was less than the total assay time, Vero cells were washed in microtiter plates and fresh medium added. With Jurkat cells the toxin/conjugate exposure was performed in centrifuge tubes which were later spun, the pellet washed, and the cells resuspended in 96-well microtiter plates in fresh medium. Because the potency of DT and DT conjugates varies from day to day on tissue culture cells, as much as a factor of 10, most of the data on protein synthesis inhibition displayed in a single figure were collected on a single day. If collected on separate days the two DT reference curves or points are provided. IC₅₀ tabular values are provided which span many days of data collection (IC₅₀, IC₆₅, and IC₈₇ indicate the molar concentration of toxin or toxin in conjugate that reduces protein synthesis 50, 65, and 87%, respectively). These tables are provided for ease in assimilating the large amount of data and the range of DT IC₅₀ values is provided to indicate the validity of comparisons.

RESULTS

Acid-catalyzed Cleavage of Anti-CD5 Diphtheria Toxin Conjugates Constructed with Cleavable Ketal Cross-linkers—Each cross-linker is identified by a number. All numbers following the term "cleavable conjugate" will identify the cleavable cross-linker in the conjugate synthesis. A detailed hydrolytic study of cleavable conjugate 2 at pH 5.5, 6.5, and 7.5 is presented in Fig. 2. The hydrolysis is observed to be first order. The half-times of hydrolysis increase 10-fold with each unit increase in pH. The half-times of hydrolysis for cleavable conjugates 1 and 3 at pH 6.5 were determined by similar methodology and are listed in Table I. Conjugate 1 is 1.5-fold faster than conjugate 2 while the hydrolytic rate of conjugate 3 is 15% of conjugate 2.

Enhancement of Potency of Anti-CD5 Conjugates with Cleavable Cross-linkers—The enhancement of potency of conjugates made with cleavable cross-linkers is shown in Figs. 3–8. In Fig. 3 the ability of anti-CD5 diphtheria toxin conjugates to inhibit protein synthesis is compared for conjugates made

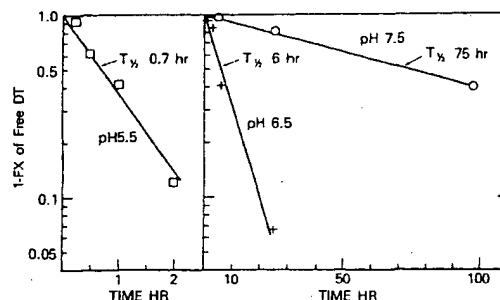


FIG. 2. Anti-human CD5 was conjugated to diphtheria toxin via the cleavable cross-linker 2 as described under "Materials and Methods." The conjugate was exposed to phosphate buffers at the indicated pH for various times, treated with 1% SDS and immediately chromatographed on GF-450 size exclusion column (Du Pont-New England Nuclear) in 0.1% SDS, pH 8.5. The fraction of free DT was determined by integration of the fractional release of DT normalized to the maximum release of DT. This value was subtracted from 1 and plotted on the ordinate to give the fraction of remaining conjugate. Half-times of hydrolysis are interpolated from the log linear plots.

TABLE I

Half-times of hydrolysis at pH 6.5 of anti-CD5 diphtheria toxin conjugates made with acid-cleavable ketal cross-linkers

Cross-linker ^a	<i>t</i> _{1/2} ^b
1	h
2	4
3	6
	40

^a Cross-linker structures are shown in Fig. 1.

^b See "Materials and Methods" for determination of *t*_{1/2} values.

with acid-cleavable and non-cleavable cross-linkers. Data are presented for both CD5 bearing target cells (Jurkat) and non-target cells (Vero) devoid of CD5. The cleavable conjugate 2 (bis-maleimidoethoxy propane) is 10–50-fold more potent toward target cells than those made with the non-cleavable cross-linkers in both 5- and 24-h assays.

The potency of cleavable conjugate 2 exceeds that of DT by a factor of 10 or greater on target cells. The enhancement of potency cannot therefore be the result of extracellular hydrolysis and the release of extracellular DT during the assay. The potency of the cleavable conjugate is reduced 100-fold by competition with excess anti-CD5 (data not shown). The enhancement is therefore unique to the CD5 uptake route. The anti-CD5 conjugate made with cleavable conjugate 4 exhibits the same dose-response curve as the conjugate made with the commercially available non-cleavable cross-linker, SMPB. The curves are shallow and protein synthesis does not decrease below the 40% value even after 24-h. Cross-linker 4 differs from cross-linker 2 in three respects: it is an acetal rather than a ketal; its construction is heterobifunctional; and its half-time of hydrolysis at pH 5.5 is 130 h compared to 0.7 for cross-linker 2. These data are summarized in Table II by listing IC₅₀ values.

The toxicity of the anti-CD5 diphtheria toxin conjugates to non-target cells (Vero) is also shown in Fig. 3 (right panels). Here intoxication can only proceed via the DT receptor and uptake route. Conjugation of DT with antibody markedly reduces DT toxicity, IC₅₀ values are increased 160- and 550-fold for the non-cleavable cross-linkers BMH and SMPB, respectively. The slowly cleavable cross-linker 4 is similar to SMPB. These heterobifunctional conjugates are less toxic than the homobifunctional BMH conjugate which more closely resembles cleavable conjugate 2 in structure. Changes

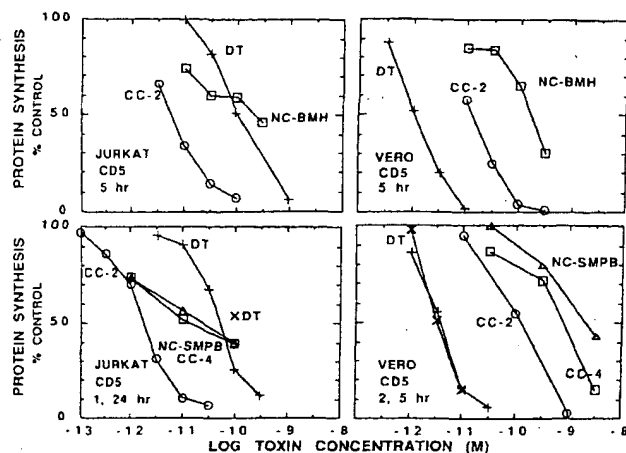


FIG. 3-8. Each panel compares the inhibition of protein synthesis by wild-type or mutant diphtheria toxin-based immunotoxins to a diphtheria toxin reference curve for that experiment labeled DT. Immunotoxins made with cleavable cross-linkers are labeled CC-#, the number indicating the cross-linker shown in Fig. 1. Non-cleavable conjugates are labeled NC-BMH when constructed with bis-maleimido-hexane or NC-SMPB (see "Materials and Methods"). The cell type used in the assay is indicated in the lower left of each panel. Below this is listed the immunotoxin targeting epitope and then the exposure time to toxin/immunotoxin followed by the total assay time. One number indicates that exposure time equals assay time. Jurkat cells are target cells for anti-CD3 and anti-CD5 immunotoxins and contain high levels of transferrin receptor (12). Colo 38 are target cells for HMW-MAA. Vero cells do not express these epitopes (with the exception of the transferrin receptor) and are used as non-target cells. When immunotoxins are constructed with mutant toxins the mutant is listed after the cross-linker.

FIG. 3. Anti-CD5 diphtheria toxin conjugates made with cleavable cross-linker 2 (○—○) and non-cleavable bis-maleimido-hexane (□—□) are assayed on Jurkat target cells for 5 h (top left) and non-target Vero cells (top right); +—+, diphtheria toxin. Bottom left, same cleavable conjugate assayed for 24 h (○—○) and compared with the non-cleavable SMPB conjugate (△—△) and the slowly cleavable conjugate made with cross-linker 4 (△—△). +—+, DT reference for ○—○. ×, DT reference for □—□, △—△. Bottom right, same conjugates as bottom left assayed on Vero cells for 2 h, followed by a wash and a 5-h exposure.

in cross-linker flexibility have been suggested to cause varying interactions of conjugate domains with cell receptors with resultant toxicity changes (28). Cleavable conjugate toxicity results on non-target cells are discussed in the following section.

Effect of Varying Cleavable Conjugate Hydrolytic Rates with Anti-CD5 Conjugates—The failure of cross-linker 4 to enhance anti-CD5 potency suggested that the hydrolytic rate of the acid-catalyzed cleavable cross-linker constituted a major variable in the enhancement process. We therefore synthesized a number of ketal cross-linkers of varying hydrolytic rates. Ketal hydrolytic rates can be increased through bulky substituents or by stabilizing the transition state which has considerable carbonium ion character by increased electron donation (29). Based on parent compounds, the hydrolytic rate of cross-linker 1 was expected to be 4-fold faster than cross-linker 2, and cross-linker 3 was expected to be 13% of cross-linker 2 (29). We determined the half-time of hydrolysis at pH 6.5 of anti-CD5 diphtheria toxin made with cross-linker 1 to be 4 h (1.5 times faster than conjugate 2) and for the cross-linker 3 conjugate 40 h (15% of the rate of cross-linker 2) (Table I).

The dose-response curve of anti-CD5 diphtheria toxin conjugates made with cross-linker 1 (Fig. 4, top left) is shifted to lower concentrations by 65% compared with cleavable conju-

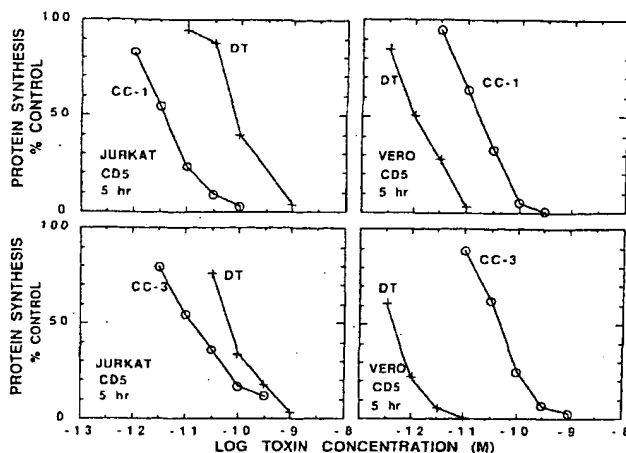


FIG. 4. Anti-CD5 diphtheria toxin conjugate made with cleavable linker 1 (○—○) assayed on Jurkat (top left) and Vero cells (top right) for 5 h; +—+, DT reference. Analogous conjugates made with cleavable cross-linker 3 assayed on Jurkat (bottom left) and Vero (bottom right) for 5 h. Symbols as on top.

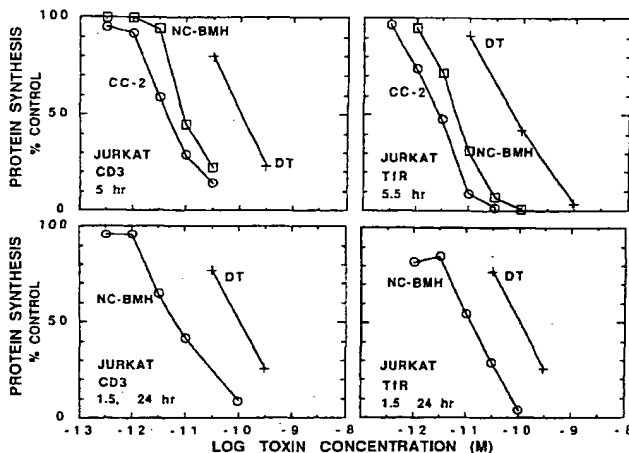


FIG. 5. Top left, anti-CD3 diphtheria toxin conjugate made with cleavable linker 2 (○—○) compared with the non-cleavable BMH linker (□—□) assayed on Jurkat cells for 5 h; +—+, reference DT. Top right, conjugates are human diphtheria toxin made with linker 2 (○—○) and BMH (□—□) assay on Jurkat cells for 5.5 h; +—+, DT reference. Bottom, BMH conjugates shown above are assayed for a 1.5-h exposure followed by a 24-h incubation. Left, anti-CD3 BMH conjugate (○—○). +—+, DT reference. Right, transferrin BMH conjugate (○—○).

gate 2. This enhancement of potency was consistently noted. On the other hand, the conjugate built with cross-linker 3 (slower hydrolytic rate constant) displays a dose-response curve with a pronounced shift in the opposite direction. The slope of the conjugate 3 curve is distinctly shallow compared with the conjugate 1 curve, although not as shallow as the non-cleavable cross-linker conjugate curves displayed in Fig. 3, left top and bottom.

When assayed on non-target cells, cross-linker 1 and 2 conjugates after a 5-h exposure exhibit similar inhibition curves. Free DT released during this assay is calculated to reach 9 and 6% of the input conjugates for conjugates 1 and 2 utilizing rate constants of 0.0187 and 0.0125 h⁻¹, respectively. When the exposure time of conjugate 2 is reduced from 5 to 2 h (Fig. 3, bottom right) the IC₅₀ value increases 3.3-fold. The cleavable conjugate is now only 2–3 times more potent than the non-cleavable BMH analog (see Table III). Similar

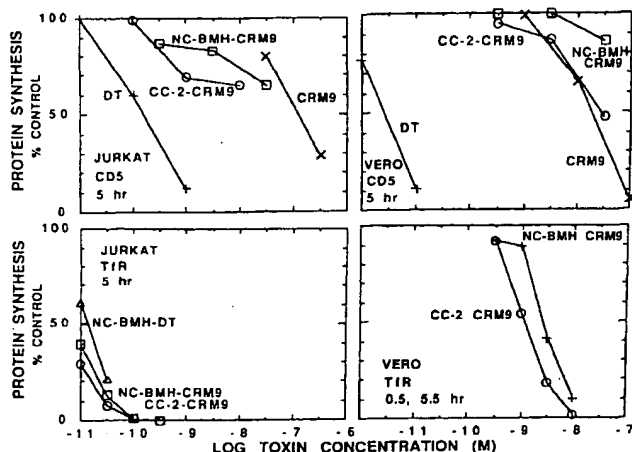


FIG. 6. *Top left*, anti-CD5-CRM9 conjugate made with cleavable linker 2 (○—○) and the non-cleavable linker BMH (□—□) are compared with CRM9 (×—×) and DT (+—+) on Jurkat cells for 5 h. *Top right*, same materials and same symbols assayed on Vero cells for 5 h. *Bottom left*, human diphtheria toxin conjugate made with the non-cleavable BMH linker (Δ—Δ) is compared with transferrin-CRM9 conjugate with the BMH linker (□—□) and transferrin CRM9 conjugate with cleavable linker 2 (○—○) on Jurkat cells for 5 h. *Bottom right*, transferrin CRM9 conjugates made with BMH and the cleavable linker 2 are assayed on Vero cells for 5.5 h following a 0.5-h exposure.

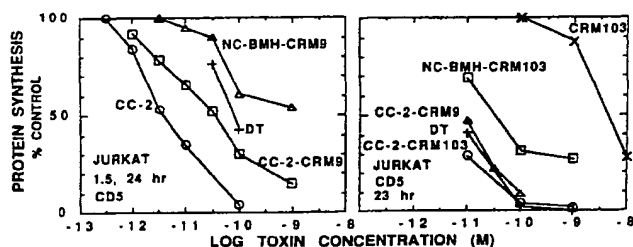


FIG. 7. *Left*, anti-CD5 cleavable conjugate 2 (○—○) is compared with the analogous conjugate made with CRM9 (□—□) and the non-cleavable BMH conjugate made with CRM9 (Δ—Δ) for a 1.5-h exposure and 24-h assay. +—+, DT reference. *Right*, anti-CD5 cleavable conjugate 2 made with CRM103 (○—○) is compared with the analogous conjugate made with CRM9 (Δ—Δ) and the non-cleavable conjugate made with BMH and CRM103 (□—□); +—+, DT reference; ×—×, CRM103. Exposure and assay are 23 h.

data were obtained for cleavable cross-linker 1 conjugate (not shown). Our interpretation is that when exposure time to the medium is reduced there is less hydrolysis of input conjugate to free toxin and consequently lower toxicity. Cleavable conjugate 3 is calculated to only release 1% of its input DT in 5 h ($k = 0.002 \text{ h}^{-1}$). In Fig. 4 (*bottom right*) it is apparent that the dose-response of cleavable conjugate 3 matches that of the non-cleavable BMH conjugate (Fig. 3, *top right*). This lack of enhancement of toxicity on non-target cells should be contrasted to the 13-fold enhancement on target cells of cleavable conjugate 3 over the BMH conjugate (Fig. 3, *top left*) $\text{IC}_{50} = 1.8 \times 10^{-10} \text{ M}$ and cleavable conjugate 3 (Fig. 4, *bottom left*) $\text{IC}_{50} = 1.4 \times 10^{-11} \text{ M}$.

To summarize the data, the ratio of the enhancement of the cleavable ketal conjugates over the non-cleavable BMH conjugate in target cells to the enhancement in non-target cells is at least 10-fold. While this fact may seem perplexing it is in keeping with the main observations of this work; there are wide variations between the toxicity of cleavable and non-

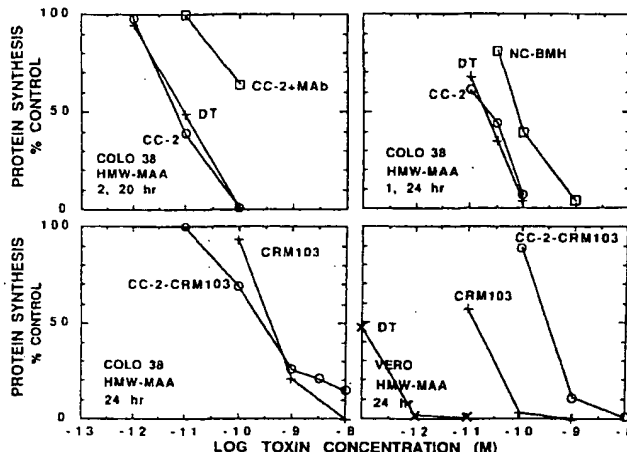


FIG. 8. *Top left*, HMW-MAA diphtheria toxin conjugate made with cleavable linker 2 (○—○). The same conjugate assayed in the presence of 10^{-6} M of the parent anti-HMW-MAA monoclonal antibody (□—□) on Colo 38 cells for 20 h after a 2-h immunotoxin exposure. *Top right*, same immunotoxin (○—○) compared with the non-cleavable BMH analog (□—□) for a 24-h assay and 1-h exposure; +—+, DT reference. *Bottom left*, anti-HMW-MAA mutant toxin CRM103 conjugate made with cleavable linker 2 (○—○) compared with CRM103 (+—+) on Colo 38 cells for 24 h. *Bottom right*, anti-HMW-MAA CRM103 conjugate constructed with linker 2 (○—○) compared with CRM103 and DT (+—+) on Vero cells for 24 h (×—×).

TABLE II

Selected data summary, Figs. 3–6

IC_{50} values are provided for inhibition of protein synthesis by toxin conjugates and toxins utilizing various cross-linkers. See Fig. 3 legend for nomenclature.

Jurkat cells		5-hr assay, IC_{50} M
Conjugate or toxin	Cross-linker	
Anti-CD5-DT	NC-BMH	2×10^{-10}
Anti-CD5-DT	CC-1	4×10^{-12}
Anti-CD5-DT	CC-2	5×10^{-12}
Anti-CD5-DT	CC-3	1×10^{-11}
Anti-CD3-DT	NC-BMH	7×10^{-12}
Anti-CD3-DT	CC-2	4×10^{-12}
Transferrin-DT	NC-BMH	1×10^{-11}
Transferrin-DT	CC-2	3×10^{-12}
Anti-CD5-CRM9	NC-BMH	$>5 \times 10^{-8}$
Anti-CD5-CRM9	CC-2	$>1 \times 10^{-8}$
Transferrin-CRM9	NC-BMH	7×10^{-12a}
Transferrin-CRM9	CC-2	3×10^{-12a}
DT		$0.5\text{--}1.0 \times 10^{-10}$
CRM9		1×10^{-7}

^a Extrapolated value.

cleavable toxin conjugates that are uniquely dependent on the conjugate uptake route.

Correlation between Cleavable Anti-CD5 Conjugate Hydrolytic Rates and Protein Synthesis Inhibition—In Fig. 9 we have plotted the target cell inhibition of protein synthesis (ordinate, log scale) versus the first-order rate constant of conjugate hydrolysis at pH 6.5 for conjugates made with the three ketal cross-linkers. Plots are made at four concentrations of input conjugates. The data are from Fig. 3, *top left*, and Fig. 4, *left top* and *bottom*. The DT reference curves of these three experiments are not significantly different and therefore these conjugates may be compared. The lines connecting points are least squares regression fit of the form $y = M_0 e^{-M_1 x}$ where y is the value of % control protein synthesis and x is the first-order rate constant. The correlation coefficient

TABLE III

Selected data summary (Figs. 3–8): anti-CD5 DT conjugates on non-target (Vero cells)

IC₅₀ values are provided for inhibition of protein synthesis by toxin conjugates and toxins utilizing various cross-linkers. See Fig. 3 legend for nomenclature.

Conjugate or toxin	Cross-linker	IC ₅₀		Assay time
		M	h	
anti-CD5-DT	NC-SMPB	2×10^{-9}	2, 5	
anti-CD5-DT	NC-BMH	2×10^{-10}	5	
anti-CD5-DT	CC-4	7×10^{-10}	2, 5	
anti-CD5-DT	CC-3	5×10^{-11}	5	
anti-CD5-DT	CC-2	2×10^{-11}	5	
anti-CD5-DT	CC-1	2×10^{-11}	5	
DT		4×10^{-12}	2, 5	
DT		1×10^{-12}	5	
CRM9		2×10^{-8}	5	

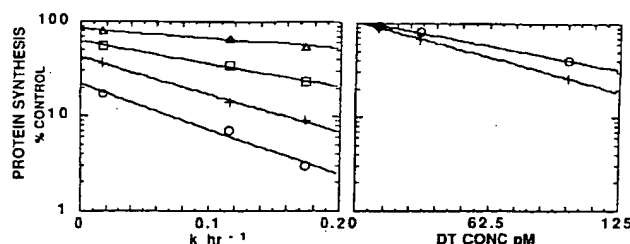


Fig. 9. Right, protein synthesis as % control after a 5-h assay is plotted on a log scale on the ordinate versus the first-order rate constant for conjugate hydrolysis, k , for cross-linkers 1, 2, and 3 determined at pH 6.5. Plots are done at four conjugate concentrations; \circ — \circ , 100 pM; $+$ — $+$, 30 pM; \square — \square , 10 pM; \triangle — \triangle , 3 pM. The lines are least square regression fits with the following correlation coefficients; 0.995, 0.999, and 0.991 ordered from 100 to 3 pM. The protein synthesis data is taken from Figs. 3 and 4. The rate constants were calculated from the half-times of hydrolysis listed in Table I. Left, ordinate is the same as in the right panel. The abscissa is DT concentration. The assay time is 5 h exposure and assay (\circ — \circ) and 1-h exposure followed by 24 h ($+$ — $+$). Lines are least square regression fits with correlation coefficients of 0.9989 and 0.9998, respectively.

cients range from 0.99 to 0.999. The rationale for this type of plot is that inactivation of protein synthesis by diphtheria toxin is a first-order process (30). This is shown in Fig. 9, right, where under two different time periods of incubation percent inhibition of protein synthesis is plotted versus toxin concentration. The points are fitted as before, only x is now diphtheria toxin concentration. (The toxin concentration range is kept below toxin receptor saturation to preserve the first-order nature of the process (7).) Taken together these graphs suggest a relationship between cleavable conjugate first-order rate constant and the effective diphtheria toxin concentration intoxicating cells via the CD5 uptake route.

Acid-cleavable Cross-linkers Provide Minimal Enhancement for Transferrin Conjugates and Anti-CD3 Conjugates—We have shown that cleavable cross-linkers make anti-CD5 diphtheria conjugates very potent; IC₅₀ values for protein synthesis inhibition are in the vicinity of 10^{-11} M after only 5 h of exposure. Anti-CD3 diphtheria toxin conjugates and transferrin conjugates made with non-cleavable cross-linkers exhibit similar potencies. It was of some interest, therefore, to see if these systems could be further enhanced by cleavable cross-linkers. The CD3 and transferrin delivery systems are also of interest because they are equally potent for wild-type diphtheria toxin conjugate and mutant toxin conjugate which have as much as $1/5000$ reduced DT receptor binding (16, 17).

We find a 2–3-fold enhancement of anti-CD3 diphtheria toxin conjugates made with cross-linker 2 over BMH when

assayed for 5 h on Jurkat cells (Fig. 5, top left; also see Table II). With transferrin conjugates the cleavable conjugates are also consistently 2–3-fold more potent (Fig. 5, top right). This is in contrast to the 10–50-fold enhancement seen with anti-CD5 conjugates constructed with cleavable cross-linkers. On non-target cells anti-CD3 conjugates made with cross-linker 2 exhibit dose-response curves similar to those of the analogous anti-CD5 conjugate (data not shown).

When the anti-CD3 non-cleavable conjugate was exposed to cells for only 1.5 h, washed, and then assayed 24 h later, we see that the toxicity (Fig. 5, left bottom) is comparable with the 5-h exposure and assay (Fig. 5, left top). A similar assay with the transferrin non-cleavable conjugate revealed a diminution of toxicity over the 5-h exposure and assay. These findings are in contrast to the anti-CD5 system where the potency of a conjugate exposed to cells for 1 h and assayed 23 h later exceeds by 3-fold the 5-h exposure and assay (data not shown). The behavior of the transferrin system may be related to the transferrin receptor functioning as a high speed shuttle moving transferrin into and out of the cell (32, 33).

The Effects of Substituting Toxin Mutants with Decreased Binding Affinities into Acid-cleavable Conjugates—We chose to use diphtheria toxin mutants with decreased binding affinities to probe the mechanism of toxicity enhancement observed with anti-CD5 and anti-HMW-MAA-cleavable conjugates. CRM103 has $1/100$ the binding affinity of wild-type DT on Vero cells (16) while CRM9 binding is $1/1000$ of wild-type DT (20). CRM103 and CRM9 exhibit $1/100$ and $1/7000$ the toxicity of wild-type DT on Vero cells, respectively (Fig. 8, bottom right; Fig. 6, top right). However both mutants exhibit equal toxicity on Jurkat cells, $1/700$ of wild-type toxins (Fig. 6, top left; Fig. 7, right).

Our rationale for constructing mutant conjugates was as follows: if the assumption is made that the toxicity enhancement of cleavable conjugates is due to release of DT free from the steric constraints of the antibody within acidic intracellular vesicles, then toxins with various binding affinities become probes for a putative intracellular receptor interaction along the processing and translocation pathway. If the steric constraints are independent of an internal DT receptor interaction, then the mutant toxins should be indistinguishable from wild-type toxins. On the other hand, if steric constraints are operative via the DT receptor (or similar interaction involving the toxin binding site) enhancement would be expected to follow the rank order for affinity: wild-type > CRM103 = CRM9 (assumed from toxicity data on Jurkat cells).

The anti-CD5 system with CRM9 is shown in Fig. 6, top left, and tabulated in Table IV. (Note the scale change on the log toxin concentration axis.) The cleavable CRM9 conjugate has no measurable toxicity after 5 h at 10^{-10} M conjugate input. At the same concentration and time cleavable CRM103 conjugate exhibits 42% of control protein synthesis (data not shown). However, the analogous wild-type conjugate (Fig. 3, top left) exhibits 7% of control protein synthesis at 10^{-10} M after 5 h. In contrast, after 5 h, CRM9 transferrin conjugates are as active as wild-type conjugates and exhibit high potency on Jurkat cells (Fig. 6, bottom left). In this system CRM9 has similar properties previously reported for CRM107 and CRM103 (16, 17). The cleavable cross-linker enhancement of the transferrin-CRM9 conjugate is less than 3-fold. The high potency of this system is related to cell type as shown by the same conjugates assayed on Vero cells, Fig. 6, bottom right. However, even in this low potency transferrin uptake system, the cleavable conjugate shows minimal enhancement over the non-cleavable analog.

TABLE IV

Data summary (Fig. 7): anti-CD5-CRM103 and CRM9 conjugates on Jurkat cells

IC₅₀ values are provided for inhibition of protein synthesis by toxin conjugates and toxins utilizing various cross-linkers. See Fig. 3 legend for nomenclature.

Conjugate or toxin	Cross-linker	IC ₅₀		Assay time
		M	h	
Anti-CD5-CRM9	NC-BMH	$>1 \times 10^{-9}$	1.5, 24	
Anti-CD5-CRM9	CC-2	4×10^{-11}	1.5, 24	
Anti-CD5-DT	CC-2	4×10^{-12}	1.5, 24	
Anti-CD5-CRM103	NC-BMH	4×10^{-11}	23	
Anti-CD5-CRM103	CC-2	1×10^{-11a}	23	
Anti-CD5-CRM9	CC-2	1×10^{-11}	23	
CRM103		5×10^{-9}	23	
DT		7×10^{-12b}	23	
DT		8×10^{-11}	1.5, 24	

^a Anti-CD5-CRM103 with CC-2 IC₅₀ value not significantly different from anti-CD5-CRM9.

^b Extrapolated value

Mutant anti-CD5 conjugates are compared after a 1.5-h exposure to target cells followed by a wash and assay after 23 h of incubation in Fig. 7, *left*. In spite of the short conjugate exposure, toxicity is substantial after 23 h of incubation. The non-cleavable BMH CRM9 and CRM103 conjugates are the least toxic. Construction of the CRM9 conjugate with cleavable linker 3 does not increase toxicity over the BMH conjugate (data not shown). However, construction with cleavable cross-linker 2 increases the potency of CRM9 and CRM103 conjugates 6-fold over the BMH conjugate, and these cleavable conjugates are equipotent (Fig. 7, *right*) after 23 h. They are also equipotent in the 1.5-h exposure 24-h assay (data not shown). The analogous cleavable wild-type conjugate displays another 10-fold increase in potency over the mutant cleavable conjugates (Fig. 7, *left*). Since these mutations involve the toxin binding site, the strong inference is that the enhancement provided by the wild-type toxin acts via a toxin-toxin receptor interaction.

Acid-cleavable Cross-linkers Enhance Anti-high Molecular Weight Melanoma-associated Antigen Conjugates—Because conjugate toxicity with mutant *versus* wild-type toxins and cleavable *versus* non-cleavable cross-linkers varied markedly with uptake route, we decided to explore uptake via HMW-MAA. Preliminary kinetic studies showed that the inactivation rate of protein synthesis inhibition at 10^{-10} M is slower with anti-HMW-MAA diphtheria toxin cleavable 2 conjugates ($0.1 \log h^{-1}$ compared with $0.25 \log h^{-1}$ for the analogous anti-CD5 conjugate (data not shown). The anti HMW-MAA is cleared less rapidly than anti-CD5 conjugates from the surface membrane as determined by adding antitoxin serum at various times after a 1-h pulse exposure to conjugates. (Colo 38 cells require 4 h prior to addition of antitoxin to express 95% of the conjugate toxicity in contrast to 1 h for either DT toxicity or anti-CD5-cleavable conjugate 2 toxicity on Jurkat cells, data not shown.)

Anti-HMW-MAA diphtheria toxin made with cleavable cross-linker 2 exhibits an IC₅₀ on Colo 38 target cells at $\sim 10^{-11}$ M after 24 h (Fig. 8, *top panels*, and Table V). These dose-response curves are nearly identical to that of DT. The cleavable conjugate is 3–10-fold more potent than the non-cleavable BMH conjugate (Fig. 8, *top right*). Although the cleavable conjugate has equal toxicity to DT, the uptake route is mainly via the HMW-MAA receptor because antibody conjugation greatly diminishes the DT receptor-mediated toxin route. This is substantiated by the 30-fold increase in IC₅₀ value on competition with excess (10^{-6} M) anti-HMW-MAA monoclonal antibody (Fig. 8, *top left*). (In this figure

TABLE V

Selected data summary of Fig. 8: anti-HMW-MAA conjugates on COLO 38 cells

IC₅₀ values are provided for inhibition of protein synthesis by toxin conjugates and toxins utilizing various cross-linkers. See Fig. 3 legend for nomenclature.

Conjugate or toxin	Cross-linker	IC ₅₀		Assay time
		M	h	
Anti-HMW-MAA-DT	NC-BMH	7×10^{-11}	1, 24	
Anti-HMW-MAA-DT	CC-2	7×10^{-12}	2, 20	
Anti-HMW-MAA-DT + excess anti-HMW-MAA	CC-2	3×10^{-10a}	2, 20	
Anti-HMW-MAA-CRM103	CC-2	3×10^{-10}	24	
CRM103		4×10^{-10}	24	

^a Extrapolated value.

the IC₅₀ comparison is made in order to avoid comparisons made between data extrapolated beyond bracketing data points.)

In the case of the anti-HMW-MAA (Fig. 8, *left*, and Table V), we see that the CRM103-cleavable conjugate has $\frac{1}{10}$ the potency of the wild-type conjugate. We lacked sufficient antibody to make a more detailed study of this system. The combination of reduced mutant conjugate toxicity compared with wild-type and a 6-fold increase in toxicity of the cleavable conjugate over the non-cleavable conjugate places the HMW-MAA system closer to the CD5 uptake system rather than the CD3 and transferrin uptake systems. These data show that wild-type and mutant diphtheria toxin conjugates have toxicities that are in large part determined by the epitope initiating the cellular uptake.

DISCUSSION

The data presented show that cleavable ketal cross-linkers 1, 2, and 3 enhance the potency and efficacy of anti-CD5 diphtheria toxin conjugates beyond that achieved with non-cleavable cross-linkers. For the three ketal cross-linkers enhancement is correlated with the experimentally determined first-order rate constant of conjugate hydrolysis at pH 6.5. The correlation is seen when the log % control protein synthesis values, obtained over a range of conjugate concentrations, are plotted *versus* experimentally determined conjugate hydrolytic rate constants (Fig. 9, *left*). This plot may be regarded as analogous to a plot of log % control protein synthesis *versus* diphtheria toxin concentration shown in Fig. 9, *right*. The log linear relation observed is expected for any dose-dependent single hit killing or inhibition process which is operating below receptor saturation (7).

We think that the simplest explanation for these correlations is that after antibody-directed receptor-mediated uptake the cleavable conjugates are hydrolyzed in part to free toxin and antibody; at any given time the amount of intracellular hydrolysis is proportional to the first-order rate constants measured at pH 6.5; free intracellular toxin released after importation via CD5 is more potent than conjugated toxin imported via CD5.

We do not know the rates of hydrolysis of these cleavable antibody conjugates within acidified intracellular compartments. We can think of no reason why the rates might be significantly slower than our experimentally determined rate constants. However, the rates could be faster because acetals and ketals are subject to local anionic effects. An example is catalysis by anionic detergents. Suggested mechanisms are 1) stabilization of the developing carbonium ion transition state; 2) locally increased concentration of hydronium ions in the vicinity of the substrate-detergent complex; 3) general acid catalysis by the protonated detergent (22). Similar effects

could be mediated at membrane vesicle interfaces. In addition, it is possible that heterogeneity exists in the hydrolytic rates due to the relatively random nature of the toxin antibody cross-linking process and subsequent secondary local anionic effects. Our method of determining hydrolytic rate yields only the bulk rate and does not distinguish faster rates comprising 5% or less of the substrate.

We have, however, acquired direct data utilizing conjugates radiolabeled in the toxin moiety, demonstrating hydrolysis of cleavable antibody-toxin conjugates within a prelysosomal compartment.³ The interpretation of these studies is complicated by the fact that diphtheria toxin undergoes processing to lower molecular weight components within acidic vesicles.³ We have also obtained direct evidence for prelysosomal hydrolysis of cleavable transferrin conjugates where it has been possible to determine the fraction of conjugate cleaved per transferrin cellular transit.⁴ These results will appear in future publications.

The results of the conjugate toxicity studies, made with cleavable and non-cleavable conjugates utilizing mutant and wild-type diphtheria toxin, reveal a pattern dictated by uptake route. Anti-CD3 and transferrin conjugates fall into one group. Potency is high with these non-cleavable conjugates. Cleavable conjugates provide minimal potency enhancement (2-3-fold), and toxin mutants, compromised in surface receptor binding, are equipotent to wild-type toxins as described previously (16, 17).

Anti-CD5 and anti-HMW-MAA conjugates are a second group. Potency of non-cleavable conjugates is low relative to the first group. Substituting a cleavable cross-linker for the non-cleavable cross-linker enhances potency 10-fold or more. Substituting a toxin binding mutant reduces potency to 10% of the wild-type toxin with a cleavable cross-linker.

Both toxin binding mutants CRM9 and CRM103 behaved similarly on Jurkat cells alone or in anti-CD5 conjugates. The mutation in CRM9 leading to reduced binding has not yet been characterized. However, CRM103 contains a single amino acid replacement of serine with phenylalanine at position 508 in the C terminus of the toxin, and this mutation results in a binding affinity equal to 1% of the wild-type toxin (16). Our results show that serine 508 is required for maximal conjugate toxicity when uptake occurs via CD5 or HMW-MAA. The inescapable inference is that the DT toxin receptor or a similar structure aids in mediating efficient toxicity after uptake via the alternate receptor. Two different membrane-associated DT binding structures of varying molecular size have been identified (34). However, individual roles in the toxicity process have not been elucidated.

The toxicity enhancement going from an anti-CD5 non-cleavable conjugate to a cleavable conjugate with mutant toxins needs explanation. We favor the same explanation as above, namely interaction with an internal toxin receptor, even though in this case potency is reduced to 10% of the wild-type conjugate, due to the reduced interaction of the mutant for the toxin receptor. The quantitative aspects of this interaction within an acidic compartment may be different from binding affinities of mutant and wild type measured at the surface membrane at pH 7.4. An alternative explanation is that the cleavable cross-linker, by reducing steric constraints, facilitates flux along the translocation pathway by a process independent of the DT receptor. However, this facilitation is not noted to this degree in uptake via CD3; nor is it

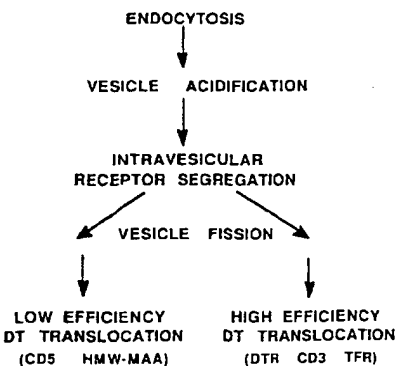


FIG. 10. Receptor segregation along the diphtheria toxin translocation pathway. One possible scheme is diagrammed which employs vesicle fission. All of the receptors under consideration are endocytosed into the same vesicles. Following acidification the routing diverges. *DTR*, *CD3*, and *TFR* (and their associated bound ligands) are segregated at one vesicular pole and *CD5* and *HMW-MAA* are segregated at the other. Following segregation but before vesicular fission DT set free by hydrolysis from a cleavable anti-CD5 or anti-HMW-MAA conjugate can become associated with free segregated DT receptors. This is the point of cross-over facilitated by the acid-cleavable cross-linker. Vesicle fission then bifurcates the pathway to compartments differing in their efficiency to translocate DT.

noted in murine cells, which lack productive toxin receptors, with anti-Thy CRM9 conjugates where toxicity is identical with cleavable and non-cleavable conjugates and equipotent to wild-type toxin conjugates.⁵

What types of mechanisms could account for the differences between CD3- and TFR-mediated toxicity versus CD5 and HMW-MAA mediated toxicity? We speculate that there are two parallel uptake routes and acid processing routes that are partially segregated. These routes can converge on or before the site of toxin membrane translocation. CD3, TFR, and the DT receptors are capable of moving conjugates (or DT toxins) to the compartment of efficient toxin translocation. Translocation *per se* does not require a DT receptor interaction. Translocation of toxin A chain into the cytosol, where the toxin meets its substrate (elongation factor 2), is not greatly hindered by conjugated antibody, or alternatively, the hindering antibody is removed by proteolytic processing within this compartment prior to translocation. Conjugate uptake via this route to non-target cells via the DT receptor is restricted by reduced binding due to steric inhibition of the toxin binding site by the conjugated antibody.

On the other hand, uptake via CD5 and HMW-MAA takes a different route and leads to a compartment that cannot efficiently translocate DT or toxin binding site mutants. Surface membrane DT receptors are not cycled through this compartment. However, the route to this compartment contains DT receptors that may or may not be identical to the surface receptors cycled together with CD3 and TFR. (Two distinct DT receptors have been identified (34).) Access to the translocating compartment can be via these DT receptors that are able to facilitate transport in some unknown way. The cleavable cross-linker enhances this interaction, more efficiently for wild-type toxin, by reducing steric hindrance in proportion to the fraction of free toxin released by hydrolysis. Thus, two effects are additive for toxicity: the degree of toxin receptor interaction and the rate of cross-linker hydrolysis. A diagrammatic representation of such a scheme is shown in Fig. 10.

The model described above has some features that are

³ D. M. Neville, Jr., K. Srinivasachar, and R. Stone, unpublished observations.

⁴ H. Wellhöner, K. Srinivasachar, and D. M. Neville, Jr., unpublished observations.

⁵ J. Marsh, personal communication.

supported by previous studies. First, there are similarities between CD3 and TfR. Both operate as shuttles between an internal compartment and the surface membrane (35, 36). Moreover, in T cells, CD3 and TfR shuttle to the same internal compartment that is associated with the microtubule organizing center (31). This compartment largely excludes CD4, CD8, and CD11 (unfortunately, CD5 was not measured) but does concentrate class I major histocompatibility complex antigens and may be involved in processing recognition reactions (31).

The degree to which these speculations fit reality awaits future clarification. What seems clear is that the requirement for a DT receptor interaction for maximal conjugate toxicity is predicated by uptake route. Where the route requires the DT receptor interaction the cleavable cross-linker provides a definite benefit by enlarging the therapeutic window between target and non-target cell toxicity. This is apparently achieved by reversibly blocking the DT receptor interaction via antibody conjugation and permitting release of this necessary function within acidified vesicles.

Our data with cross-linkers of varying hydrolytic rates indicate that conjugates made with cross-linkers with even faster hydrolytic rates would be more toxic to target cells. However, the utility of these *in vivo* is limited because of the significant amount of hydrolysis that occurs at the extracellular pH of 7.4. For example, cleavable conjugate 2 hydrolyzes to the free toxin at approximately 1%/h at this pH. Cross-linker 3 with the slowest hydrolytic rate actually gives the widest therapeutic window with wild-type toxin; however, the maximal target cell kill is compromised. The mutant toxins with the cleavable cross-linker also exhibit a wide therapeutic window but again maximum cell kill is compromised. (We are currently evaluating the *in vivo* therapeutic utility of the cleavable conjugates described in this paper utilizing Jurkat cells in a nude mouse system.) It is likely that the *in vivo* toxicity of mutant toxins can be further diminished by reducing the number of residues in the C terminus binding region without impairing toxicity via the TfR and CD3 uptake routes (8, 10); but this would reduce conjugate toxicity by uptake routes requiring DT receptor interactions. It will be essential to identify other surface receptor uptake routes that resemble the CD3 and TfR situation with respect to DT mutants and to define the responsible features.

Another aspect for future work is to find alternate methods for reversible release of essential functionalities within cellular compartments that are targeted to cells in a blocked form. Linkages with enzyme-sensitive bonds cleaved by enzymes that are localized along the translocation pathway would be a possible example. It also should be possible to design pH-sensitive cross-linking reagents that utilize cooperative interactions and therefore exhibit a reaction order greater than 1 with respect to $[H^+]$ and thereby further enlarge the therapeutic window of targeted reversibly blocked delivery systems.

Acknowledgments—We thank Randall Holmes for supplying CRM9, Neal Groman for supplying CRM103, Joseph Shiloach and the NIH Pilot Plant for growing diphtheria toxin mutants, Soldano Ferrone for the generous gift of anti-HMW-MAA and Colo 38 cells, Jon Marsh for helpful discussions, and Sandra Means for typing the manuscript. We thank Hybritech Corp. (San Diego) for the generous gift of T101 antibody.

REFERENCES

1. Chang, T., and Neville, D. M., Jr. (1977) *J. Biol. Chem.* **252**, 1505-1514
2. Frankel, A. E. (ed) (1988) *Immunotoxins*, Kluwer Academic Publishers, Dordrecht, the Netherlands
3. Robbins, A. R., Myerowitz, R., Youle, R. J., Murray, G. J., and Neville, D. M., Jr. (1981) *J. Biol. Chem.* **256**, 10618-10622
4. Filipovich, A. H., Valleria, D. A., Youle, R. J., Haake, R., Blazar, B. R., Arthur, D., Neville, D. M., Jr., Ramsay, N. K., McGlave, P., and Kersey, J. H. (1987) *Transplantation (Balto.)* **44**, 62-69
5. Neville, D. M., Jr. (1986) *CRC Crit. Rev. Ther. Drug Carrier Syst.* **2**, 329-352
6. Chang, T., Dazord, A., and Neville, D. M., Jr. (1977) *J. Biol. Chem.* **252**, 1515-1522
7. Neville, D. M., Jr., and Youle, R. J. (1982) *Immunol. Rev.* **62**, 75-91
8. Youle, R. J., Murray, G. J., and Neville, D. M., Jr. (1981) *Cell* **23**, 551-559
9. Youle, R. J., and Colombatti, M. (1987) *J. Biol. Chem.* **262**, 4676-4682
10. Leonard, J. E., Wang, Q.-C., Kaplan, N. O., and Royston, I. (1985) *Cancer Res.* **45**, 5263-5269
11. Marsh, J. W., and Neville, D. M., Jr. (1986) *Biochemistry* **25**, 4461-4467
12. Esworthy, R. S., and Neville, D. M., Jr. (1984) *J. Biol. Chem.* **259**, 11496-11504
13. Murphy, J. R. (1988) in *Immunotoxins* (Frankel, A. E., ed) pp. 123-140, Kluwer Academic Publishers, Dordrecht, the Netherlands
14. Colombatti, M., Greenfield, L., and Youle, R. J. (1986) *J. Biol. Chem.* **261**, 3030-3035
15. Myers, D. A., and Villemez, C. L. (1988) *J. Biol. Chem.* **263**, 17122-17127
16. Greenfield, L., Johnson, V. G., and Youle, R. J. (1987) *Science* **238**, 536-539
17. Johnson, V. G., Wilson, D., Greenfield, L., and Youle, R. J. (1988) *J. Biol. Chem.* **263**, 1295-1300
18. FitzGerald, D. J., Willingham, M. C., and Pastan, I. (1988) in *Immunotoxins* (Frankel, A. E., ed) pp. 161-173, Kluwer Academic Publishers, Dordrecht, the Netherlands
19. Kondo, T., FitzGerald, D., Chaudhary, V. K., Adhya, S., and Pastan, I. (1988) *J. Biol. Chem.* **263**, 9470-9475
20. Hu, V. W., and Holmes, R. K. (1987) *Biochim. Biophys. Acta* **902**, 24-30
21. Srinivasachar, K., and Neville, D. M., Jr. (1989) *Biochemistry* **28**, 2501-2509
22. Cordes, E. H., and Bull, H. G. (1974) *Chem. Rev.* **74**, 581-603
23. Laird, W., and Gorman, N. (1976) *J. Virol.* **19**, 220-227
24. Mueller, J. H., and Miller, P. A. (1941) *J. Immunol.* **40**, 21-32
25. Pappenheimer, A. M., Jr., Uchida, T., and Harper, A. A. (1972) *Immunochemistry* **9**, 891-906
26. Welkos, S. L., and Holmes, R. K. (1981) *J. Virol.* **37**, 936-945
27. Ziai, M. R., Imberti, L., Nicotra, M. R., Badaracco, G., Segatto, O., Natali, P. G., and Ferrone, S. (1987) *Cancer Res.* **47**, 2472-2480
28. Marsh, J. W., and Neville, D. M., Jr. (1988) *J. Immunol.* **140**, 3674-3678
29. Kreevoy, M. M., Morgan, C. R., and Taft, R. W., Jr. (1960) *J. Am. Chem. Soc.* **82**, 3064-3066
30. Neville, D. M., Jr., and Marsh, J. W. (1988) in *Immunotoxins* (Frankel, A. E., ed) pp. 393-404, Kluwer Academic Publishers, Dordrecht, the Netherlands
31. Tse, D. B., Al-Haideri, M., Pernis, B., Cantor, C. R., and Wang, C. Y. (1987) *Science* **234**, 748-751
32. Ciechanover, A., Schwartz, A. L., Dautry-Varsat, A., and Lodish, H. F. (1983) *J. Biol. Chem.* **258**, 9681-9689
33. Klausner, R. D., Van Renswoude, J. V., Ashwell, G., Kempf, C., Schechter, A. N., Dean, A., and Bridges, K. R. (1983) *J. Biol. Chem.* **258**, 4715-4724
34. Mekada, E., Okada, Y., and Uchida, T. (1988) *J. Cell Biol.* **107**, 511-519
35. Krangel, M. S. (1987) *J. Exp. Med.* **165**, 1141-1159
36. Minami, Y., Samelson, L. E., and Klausner, R. D. (1987) *J. Biol. Chem.* **262**, 13342-13347